Technical

Interim Report
I-A2049-32

Report

SOME REFINEMENTS OF THE THEORY OF THE VISCOUS SCREW PUMP

by

H. G. Elrod

March 1969

Prepared under

Contract Nonr-2342(00)
Task NR 062-316

Jointly Supported By

Department of Defense
Atomic Energy Commission
National Aeronautics and Space Administration

Administered by

Office of Naval Research
Department of the Navy

THE FRANKLIN INSTITUTE RESEARCH LABORATORIES
BENJAMIN FRANKLIN PARKWAY • PHILADELPHIA, PENNA. 19103

52

Technical

Interim Report
I-A2049-32

Report

SOME REFINEMENTS OF THE THEORY OF THE VISCOUS SCREW PUMP

by

H. G. Elrod

March 1959

Prepared under

Contract Nonr-2342(00)
Task NR 062-316

Jointly Supported By

Department of Defense
Atomic Energy Commission
National Aeronautics and Space Administration

Administered by

Office of Naval Research
Department of the Navy

THE FRANKLIN INSTITUTE RESEARCH LABORATORIES
BENJAMIN FRANKLIN PARKWAY • PHILADELPHIA, PENNA. 19103

ABSTRACT

Recently-performed analysis for herringbone thrust bearings has been incorporated into the theory of the viscous screw pump for Newtonian fluids. In addition, certain earlier corrections for sidewall and channel curvature effects have been simplified. The result is a single, refined formula for the prediction of the pressure-flow relation for these pumps.

To provide a self-contained presentation, some of the results of FIL Interim Report I-A2049-31 are also given here.

TABLE OF CONTENTS

LIST OF FIGURES

TABLE OF SYMBOLS
(Equation Number Indicates Where Symbol First Used)

c	Nominal film thickness, (2.03)
$f(\zeta)$	Pressure ripple function, (2.05)
$F(\zeta)$	Ripple function, (2.12)
$F(\alpha)$	Radius ratio function (Booy), (B.03)
F_k	Hyperbolic function, (A.04)
F_D, F_P	Correction factors for pump formula, (9.03)
F_{DC}, F_{PC}	Booy's correction factors, (8.01)
F_{PE}	Booy correction factor, (8.02)
g	Constant in ripple solution, (2.07)
$G(\zeta)$	Ripple function, (2.12)
G	Radius ratio function (Booy), (B.04)
h	Film thickness, (2.01)
H	Dimensionless film thickness, h/c, (2.03)
K	Radius ratio function (Booy), (B.05)
L	Axial distance (x_2) through pump, Fig. 2
$\dot{m}_{x1}, \dot{m}_{x2}$	Components of mass flux, (4.01)
$\dot{M}$	Total mass flowrate through pumping section, (4.05)
p	Pressure, (2.01)
P^*	Dimensionless pressure, (9.12)
Δp_{corr}	Muijdermann's pressure correction factor, Fig. 10
$\tilde{q}$	Homogeneous solution of eq. (2.04), (3.01)
Q	Volumetric flowrate, (5.02). Q_D due to drag. Q_P due to pressure gradient.
Q^*	Dimensionless flow, (9.12)
r	Assignable constant, (A.12)
R_o, R_1	Outer and inner radii of channel, resp., (6.01)

s	Width of channel or groove, Fig. 5
St	Sawtooth function, (2.14)
S	Filmthickness constants, (9.14)
$S(\alpha)$	Radius ratio function (Booy), (B.02)
$T(\alpha)$	Radius ratio function (Booy), (B.02)
U_1	Velocity of surface in x_1-direction, (2.01)
v	Velocity of fluid in y-coordinate system, (5.01)
v_p, v_h	Particular and homogeneous solutions of (A.01), (A.02) and (A.03)
V_2	Velocity of surface in y_2-direction, (A.02)
x_k	Cartesian coordinates, Fig. 2 and (2.01).
x	Dummy variable for cosine function, (A.14)
y_k	Coordinates for inclined Cartesian coordinate system, (2.02)
α	Pressure-gradient constant in interior solution, (2.05)
α	Radius ratio, R_1/R_0, (B.01)
β	Groove angle, Fig. 2
γ	Fraction of Δ devoted to groove or channel, (2.13)
Δ	Wavelength of groove-ridge cycle, Fig. 2
ϵ	h_G/R_0, (6.03)
ξ	Dimensionless distance in y_1-direction, scaled by (2.03)
ξ	Coordinate in complex plane, (C.02)
η	y_3/h_G, (A.01)
η	Coordinate in complex plane, (C.02)
μ	Viscosity, (2.01)
ζ	Dimensionless distance in x_2-direction, scaled by L, (2.03)
π	Dimensionless pressure, (2.03)

π	3.14159
ρ	Density, (4.02)
τ	y_1/h_G, (A.01)
ϕ_o	Groove angle at radius R_0. (Booy's notation)
ψ	Digamma function, (7.06)

I. INTRODUCTION

Figure 1 shows a schematic diagram of a viscous screw pump. This device is used to pump relatively small quantities of viscous liquid against relatively high pressure differences. It is used, for example, in the melt extrusion of plastics. In operation, as the screw rotates, the barrel surface drags by viscous shear a ribbon of liquid between the "flights" of the screw from a feed port at low pressure to a discharge port at high pressure.

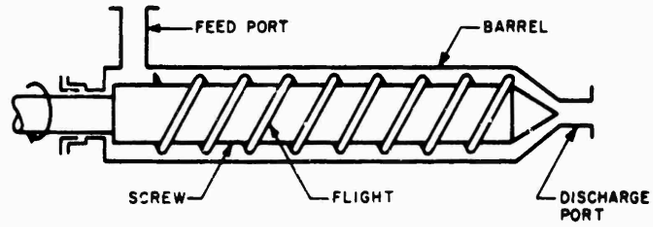

Figure 1. Schematic Diagram of Pump (adapted from ref. 2)

A substantial body of literature pertaining to the operation of the screw pump already exists, as the reader who pursues the subject will discover. The references cited herein are believed, however, to give a state-of-the-art picture of the theory of viscous screw pump operation with Newtonian fluids. The purpose of the present work has been both to generalize and to simplify some of the prior theoretical results. In particular, it has been possible to incorporate almost directly some recent analysis performed to treat herringbone thrust bearings.

The simplest theoretical treatment of the viscous screw

pump involves an "unwrapping" of the pumping channel to create a passage between parallel planes. Flow over the flight tips is neglected. The channel depth is taken as very small compared with its width, so that Reynolds' equation can be employed for computation of mass fluxes. A simple formula relating flow and operating pressure difference can thereby be obtained [5].

Successive improvements of the simplified theory are possible. For the isolated, rectangular, parallel-plate channel the effects of finite width ("sidewall effects") can be taken into account [4,6,2]. Also, for the same geometry compatibility between the interior transverse pressure ripple and uniform exterior pressures (at inlet and discharge) can be achieved [2,3]. Without unwrapping, the isolated rectangular channel of large width-to-depth aspect ratio can be analyzed for the effect of channel curvature [1]. If sidewall effects, channel curvature and entrance-exit effects are neglected, Reynolds' equation can be solved jointly for groove and ridge film thicknesses [3,7]. Moreover, variation of the channel depth in the direction of flow can be accommodated [7].

In the present work, a Reynolds' equation treatment for arbitrary transverse ridge and groove shape is given for the pump interior, and the general theory for the corresponding edge effects is set up. The edge-effect analysis is numerically implemented for the case of rectangular grooves and ridges, an exact solution being obtained in the case of an isolated groove. Simplifications of the treatment of sidewall and curvature influences are offered.

II THE INTERIOR PRESSURE SOLUTION

The starting-point for the present analysis is Reynolds' equation for a constant-property Newtonian fluid, applied to the unwrapped groove-ridge combination shown in Figure 2.

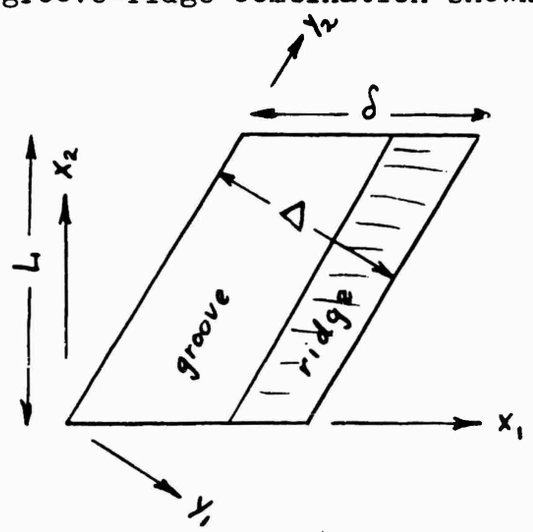

Figure 2 "Unwrapped" Groove-Ridge Combination, Showing Coordinates and Dimensions Employed

Thus:

$$U_1 \frac{\partial h}{\partial X_1} = \frac{1}{6\mu}\left\{\frac{\partial}{\partial X_1} h^3 \frac{\partial p}{\partial X_1} + \frac{\partial}{\partial X_2} h^3 \frac{\partial p}{\partial X_2}\right\} \qquad (2.01)$$

Conversion of this equation to the skewed coordinate system (Y_1, X_2) gives:

$$(\sin\beta)\, U_1 \frac{\partial h}{\partial Y_1} = \frac{1}{6\mu}\left\{\frac{\partial}{\partial Y_1} h^3 \frac{\partial p}{\partial Y_1} + \frac{\partial}{\partial X_2} h^3 \frac{\partial p}{\partial X_2} - 2(\cos\beta) h^3 \frac{\partial^2 p}{\partial Y_1 \partial X_2} - (\cos\beta) \frac{\partial p}{\partial X_2} \frac{\partial h^3}{\partial Y_1}\right\} \qquad (2.02)$$

Now take:

$$p = \frac{6\mu\Delta \sin\beta\, U_1}{c^2}\pi \qquad \zeta = \frac{Y_1}{\Delta} \qquad \xi = \frac{X_2}{L} \qquad H \equiv \frac{h}{c} \qquad (2.03)$$

Then:

$$\frac{\partial H}{\partial \zeta} = \frac{\partial}{\partial \zeta} H^3 \frac{\partial \pi}{\partial \zeta} + \left(\frac{\Delta}{L}\right)^2 \frac{\partial}{\partial \xi} H^3 \frac{\partial \pi}{\partial \xi} - 2(\cos\beta)\frac{\Delta}{L} H^3 \frac{\partial^2 \pi}{\partial \xi \partial \zeta} - \frac{\Delta}{L}(\cos\beta) \frac{\partial \pi}{\partial \xi} \frac{\partial H^3}{\partial \zeta} \qquad (2.04)$$

Asymptotically (away from inlet and exit) it is anticipated that the pressure will rise linearly with distance along the groove. Substitute the following "interior" solution

into eq. (2.04).

$$\pi = \frac{\alpha \xi}{\frac{\Delta}{L}\cos\beta} + f(\zeta) \tag{2.05}$$

An ordinary differential equation for the transverse pressure ripple, $f(\zeta)$, is thereby obtained. Thus:

$$\frac{dH}{d\zeta} = \frac{d}{d\zeta} H^3 \frac{df}{d\zeta} - \alpha \frac{dH^3}{d\zeta} \tag{2.06}$$

One integration gives:

$$H = H^3 \frac{df}{d\zeta} - \alpha H^3 + g \; ; \; g, \text{ a constant} \tag{2.07}$$

Or:

$$\frac{df}{d\zeta} = H^{-2} + \alpha - g H^{-3} \tag{2.07}$$

Since the net change in "f" over one cycle in "ζ" must be zero, "g" must satisfy the following condition.

$$0 = \overline{H^{-2}} + \alpha - g\,\overline{H^{-3}} \tag{2.08}$$

Therefore:

$$\overline{H^{-3}} \frac{df}{d\zeta} = \left(\bar{H}^2 \overline{\bar{H}^3} - \overline{\bar{H}^2}\bar{H}^3\right) + \alpha\left(\overline{\bar{H}^3} - \bar{H}^3\right) \tag{2.09}$$

Or:

$$\overline{\bar{H}^3} f(\zeta) = -\frac{1}{2} F(\zeta) - \alpha G(\zeta) \tag{2.10}$$

Where:

$$F(\zeta) = 2\int_0^{\zeta} \left(\overline{\bar{H}^2}\bar{H}^3 - \overline{\bar{H}^3}\bar{H}^2\right) d\zeta \; ; \; G(\zeta) = \int_0^{\zeta} \left(\bar{H}^3 - \overline{\bar{H}^3}\right) d\zeta \tag{2.11}$$

The "interior" pressure solution is therefore given by:

$$\pi = \frac{\alpha \xi}{\left(\frac{\Delta}{L}\cos\beta\right)} - \left\{\alpha G(\zeta) + \frac{1}{2} F(\zeta)\right\} \Big/ \overline{\bar{H}^3} \tag{2.12}$$

For rectangular geometry such that:

$$H = H_1, \; 0 \le \zeta \le r \; : \; H = H_2, \; r < \zeta < 1 \tag{2.13}$$

the pressure solution is:

$$\pi = \frac{\alpha \xi}{\left(\frac{\Delta}{L}\cos\beta\right)} - \left\{\left(\bar{H}_1^{-3}\bar{H}^{-2} - \bar{H}^{-3}\bar{H}_1^{-2}\right) + \alpha\left(\bar{H}^{-3} - \bar{H}_1^{-3}\right)\right\} \frac{\delta t(\zeta, \tau)}{\bar{H}^{-3}} \qquad (2.14)$$

Here $\delta t(\zeta, \tau)$ is the "sawtooth function" depicted in Fig. 3.

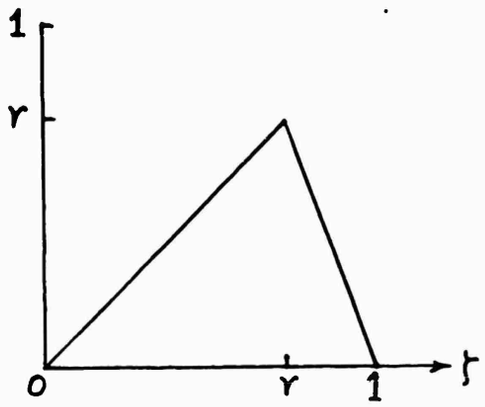

Figure 3 Sketch of the "Sawtooth Function"

III THE EDGE CORRECTION

Although solution (2.11) is an exact solution of the differential equation (2.04), and is adequate for the pump interior, it does not satisfy conditions of pressure uniformity at $\xi = 0$ and $\xi = 1$. Therefore, in accordance with standard procedure in the solution of linear differential equations, a homogeneous solution is sought which can be combined with the inhomogeneous solution to satisfy boundary conditions.

Let $\tilde{q}(\xi, \zeta)$ be a solution of the following homogeneous differential equation:

$$\frac{\partial}{\partial\zeta} H^3 \frac{\partial \tilde{q}}{\partial \zeta} + \left(\frac{\Delta}{L}\right)^2 \frac{\partial}{\partial \xi} H^3 \frac{\partial \tilde{q}}{\partial \xi} - 2(\cos\beta)\left(\frac{\Delta}{L}\right) H^3 \frac{\partial^2 \tilde{q}}{\partial \xi \partial \zeta} - \left(\frac{\Delta}{L}\right)(\cos\beta) \frac{\partial \tilde{q}}{\partial \xi} \frac{dH^3}{d\zeta} = 0 \qquad (3.01)$$

Boundary conditions on "$\tilde{q}$" appropriate to the inlet region are:

$$\tilde{q}^i(0, \zeta) = \frac{\alpha G(\zeta) + \frac{1}{2} F(\zeta)}{\bar{H}^{-3}} \qquad (3.02)$$

$$\tilde{q}^i(\xi, \zeta) \to \tilde{q}_\infty^i, \text{ a constant, as } \xi \to \infty.$$

Likewise, boundary conditions appropriate to the exit region are:

$$\tilde{q}^e(1,\zeta) = \frac{\alpha G(\zeta) + \frac{1}{2} F(\zeta)}{\overline{H^3}}$$

$$\tilde{q}^e(\chi,\zeta) \to \tilde{q}^e_\infty, \text{ a constant, as } 1-\chi \to \infty. \qquad (3.03)$$

Corresponding functions $(\tilde{q}^i - \tilde{q}^i_\infty)$ and $(\tilde{q}^e - \tilde{q}^e_\infty)$ vanish in the pump interior, but possess the required "ripple" at the exit and/or entrance. Evaluation of specific "$\tilde{q}'_\infty s$" will be deferred.

As the general solution satisfying both differential equation and boundary conditions, we have, then:

$$\pi = \frac{\alpha \chi}{\left(\frac{\Delta}{L}\cos\beta\right)} - \left\{\frac{\alpha G(\zeta) + \frac{1}{2} F(\zeta)}{\overline{H^3}}\right\} + (\tilde{q}^i - \tilde{q}^i_\infty) + (\tilde{q}^e - \tilde{q}^e_\infty) + \text{const.} \qquad (3.04)$$

The constant "α" in eq. (3.04) can be found by taking the difference between results at $\xi = 0$ and $\xi = 1$. Thus:

$$\pi(1) - \pi(0) = \frac{\alpha}{\left(\frac{\Delta}{L}\cos\beta\right)} + \tilde{q}^i_\infty - \tilde{q}^e_\infty \qquad (3.05)$$

In view of the definition of "π" and the fact that the "$\tilde{q}'_\infty s$" are independent of (Δ/L), it can be seen that, as (Δ/L) approaches zero with finite pressure difference between entrance and exit, "α" is ascertainable with increasingly high precision. In other words, the edge phenomena have vanishingly small effect on the general linear pressure rise within the pump as the groove-to-length ratio of the channels becomes small.

IV FLOWRATES ACCORDING TO REYNOLDS EQUATION

The mass flux per unit transverse distance in the x_2-direction is given, according to Reynolds' relations, by:

$$\dot{m}_{x_2} = -\frac{h^3}{12\mu}\rho\left(\frac{\partial p}{\partial x_2}\right)_{x_1} \qquad (4.01)$$

Conversion to the dimensionless variables "π, ξ, and ζ" gives:

$$\dot{m}_{x_2} = -\frac{\rho c U_1 (\sin\beta) H^3}{2}\left\{\left(\frac{\Delta}{L}\right)\frac{\partial \pi}{\partial \xi} - (\cos\beta)\frac{\partial \pi}{\partial \zeta}\right\} \qquad (4.02)$$

Since eq. (2.05) gives an accurate evaluation of "π" in the pump interior, and since the total throughput must be invariable at all axial locations, this equation is now used in (4.02). Therefore:

$$\dot{m}_{x_2} = -\frac{\rho c U_1 (\sin\beta) H^3}{2}\left\{\frac{\alpha}{(\cos\beta)} - (\cos\beta)\frac{df}{d\zeta}\right\} \qquad (4.03)$$

Use of eq. (2.09) then yields:

$$\dot{m}_{x_2} = -\frac{\rho c U_1 (\sin\beta)(\cos\beta)}{2\,\overline{H^{-3}}}\left\{\alpha\left(1 + H^3\overline{H^{-3}}\tan^2\beta\right) + \left(\overline{H^{-2}} - H\overline{H^{-3}}\right)\right\} \qquad (4.04)$$

The total mass flow per groove-ridge combination is found by integrating over a distance "δ." Thus:

$$\dot{M} = -\frac{\rho c U_1 (\cos\beta)\Delta}{2\,\overline{H^{-3}}}\left\{\alpha\left(1 + \overline{H^3}\,\overline{H^{-3}}\tan^2\beta\right) + \left(\overline{H^{-2}} - \overline{H}\,\overline{H^{-3}}\right)\right\} \qquad (4.05)$$

The pressure-discharge performance of the screw pump can now be found -- according to Reynolds' equation -- by the insertion in eq. (4.05) of the pressure-gradient value of "α" from eq. (3.05).

An alternate way of arriving at the expression for "$\dot{M}$" consists of calculating the flow components separately across lines AB and BC shown in Fig. 4. These flows combine to give "$\dot{M}$", of course, but it will be helpful for later purposes to possess this flow breakdown.

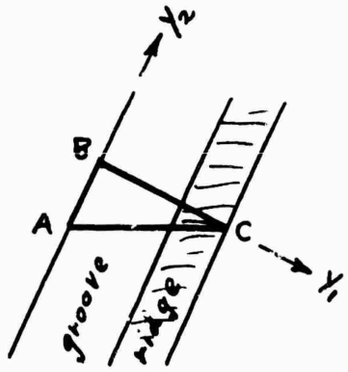

Figure 4 Control Region ABC Used for Secondary Method of Calculating Mass Flow

The mass flux in the x_1-direction is, according to Reynolds' approximations:

$$\dot{m}_{x_1} = \frac{\rho U_1 h}{2} - \frac{h^3}{12\mu} \rho \frac{\partial p}{\partial x_1} \qquad (4.06)$$

Components of the mass flux vector are now readily found in the y_1 and y_2-directions by use of eqs. (4.01) and (4.06). In particular, it is found that:

$$\int_A^B \dot{m}_{y_1} \, dy_2 = \frac{\rho c U_1 (\cos\beta)}{2} \frac{(\alpha + \bar{H}^{-2})}{\bar{H}^{-3}} \Delta \qquad (4.07)$$

and:

$$\int_B^C \dot{m}_{y_2} \, dy_1 = \frac{\rho c U_1 (\cos\beta)}{2} \{\bar{H} - \alpha \bar{H}^3 (\tan^2\beta)\} \Delta \qquad (4.08)$$

V SIDEWALL EFFECTS

Viewed in the y_2-direction, the groove-ridge cross-section within the pump appears like that in the sketch of Fig. 5 Reynolds' equation cannot take account of the fact that fluid velocities must vanish on the sides PQ and RS of this configuration. To accommodate such boundary conditions, the full Stokes' equation must be used.

There can be little doubt that even within the more precise theory of Stokes' equation, an interior region of the

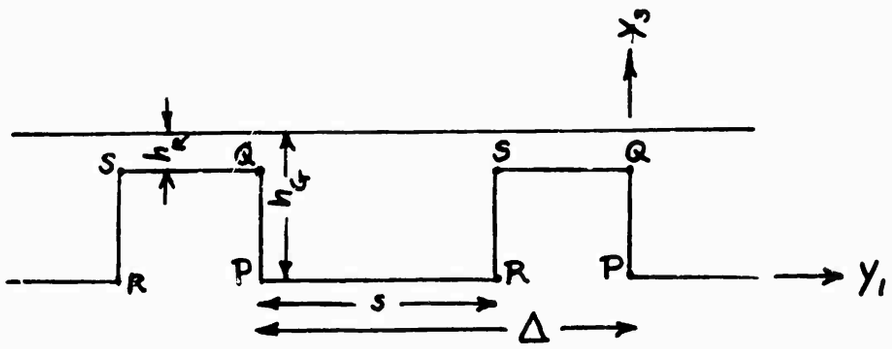

Figure 5 Groove-Ridge Cross-section

pump exists where velocity patterns are established and where $\partial p/\partial y_2$ is constant. For the coordinate system (y_1, y_2, y_3) Stokes' equation for "v_2" becomes:

$$\frac{\partial^2 v_2}{\partial y_1^2} + \frac{\partial^2 v_2}{\partial y_3^2} = -\frac{1}{\mu}\frac{\partial p}{\partial y_2} \qquad (5.01)$$

Although this is a simple form of Poisson's equation, the boundary conditions on the groove-ridge corrugations are awkward.

Since usually the ridge or flight film thickness is much less than the channel or groove film thickness, examination of the solution for an isolated groove of dimensions (h_G x s). Exact solutions have been given by a number of authors in several different forms. Here we write:

$$Q = Q_D + Q_P$$

with:

$$Q_D = \frac{V_2 h_G s}{2}\left[1 - \left(\frac{h_G}{s}\right)\frac{16}{\pi^3}\sum_{k=1,3,5}^{\infty}\frac{\tanh\left(\frac{k\pi s}{2h_G}\right)}{k^3}\right] \qquad (5.02)$$

$$Q_P = -\frac{h_G^3 s}{12\mu}\frac{\partial p}{\partial y_2}\left[1 - \left(\frac{h_G}{s}\right)\frac{192}{\pi^5}\sum_{k=1,3,5}^{\infty}\frac{\tanh\left(\frac{k\pi s}{2h_G}\right)}{k^5}\right] \qquad (5.03)$$

The series terms in the foregoing equations represent deviations from the results of Reynolds' equation. For $h_G/s \leq 3/4$,

the following approximations are accurate within 2.5%, improving very rapidly as the depth-to-width ratio diminishes. Thus:

$$Q_D = \frac{1}{2} V_2 h_G s \left[1 - 0.5428 \left(\frac{h_G}{s}\right)\right] \quad (5.04)$$

$$Q_P = -\frac{h_G^3 s}{12\mu} \frac{\partial p}{\partial y_2} \left[1 - 0.6302 \left(\frac{h_G}{s}\right)\right] \quad (5.05)$$

A derivation for the flow deficiency along the sidewalls from the groove bottom to some arbitrary position "Y_3" is given in Appendix A. For this more general case, expressions (5.04) and (5.05) become:

$$Q_D = \frac{1}{2} V_2 h_G s \left\{1 - \frac{h_G}{s} f_1\left(\frac{Y_3}{h_G}\right)\right\} \quad (5.06)$$

$$Q_P = -\frac{h_G^3 s}{12\mu} \frac{\partial p}{\partial y_2} \left\{1 - \frac{h_G}{s} f_2\left(\frac{Y_3}{h_G}\right)\right\} \quad (5.07)$$

The functions "f_1" and "f_2" are shown in Figs. 6 and 7 respectively.

The foregoing sidewall analysis is strictly applicable only to the case of an isolated (or closed) rectangular groove. However, with $\underline{PQ}/\underline{PT}$ taken as the argument (y_3/h_G) in Figs. 6 and 7, the flow deficiencies for open rectangular grooves are approximated. This particular mode of approximation will lead to somewhat greater-than-actual absolute values of both flow deficiencies, since some of the flow constraint along $\underline{QT}$ is missing in the case of the open groove.

Figure 6

SIDEWALL CORRECTION FACTOR

DRAG FLOW

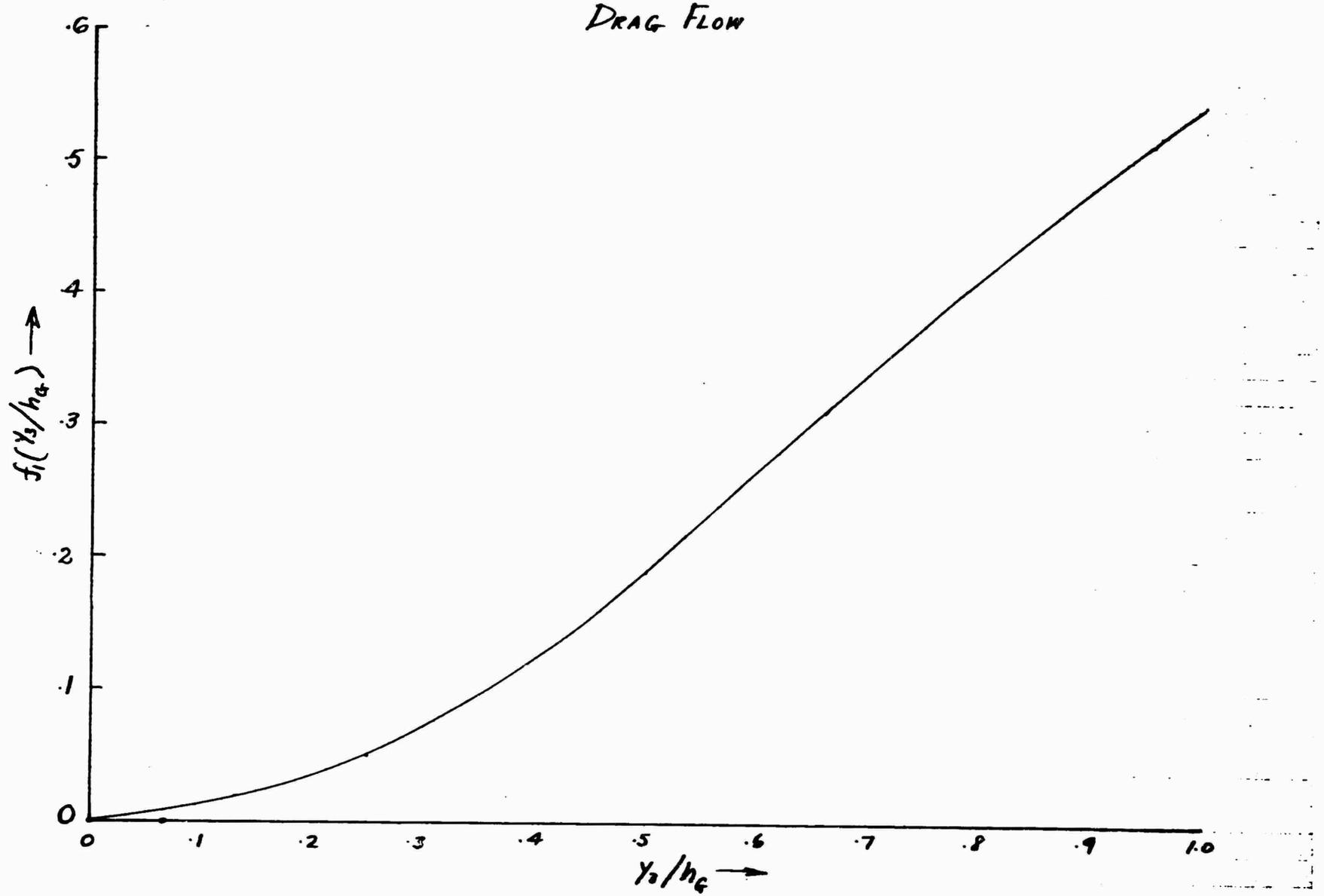

Figure 7 SIDEWALL CORRECTION FACTOR

PRESSURE FLOW

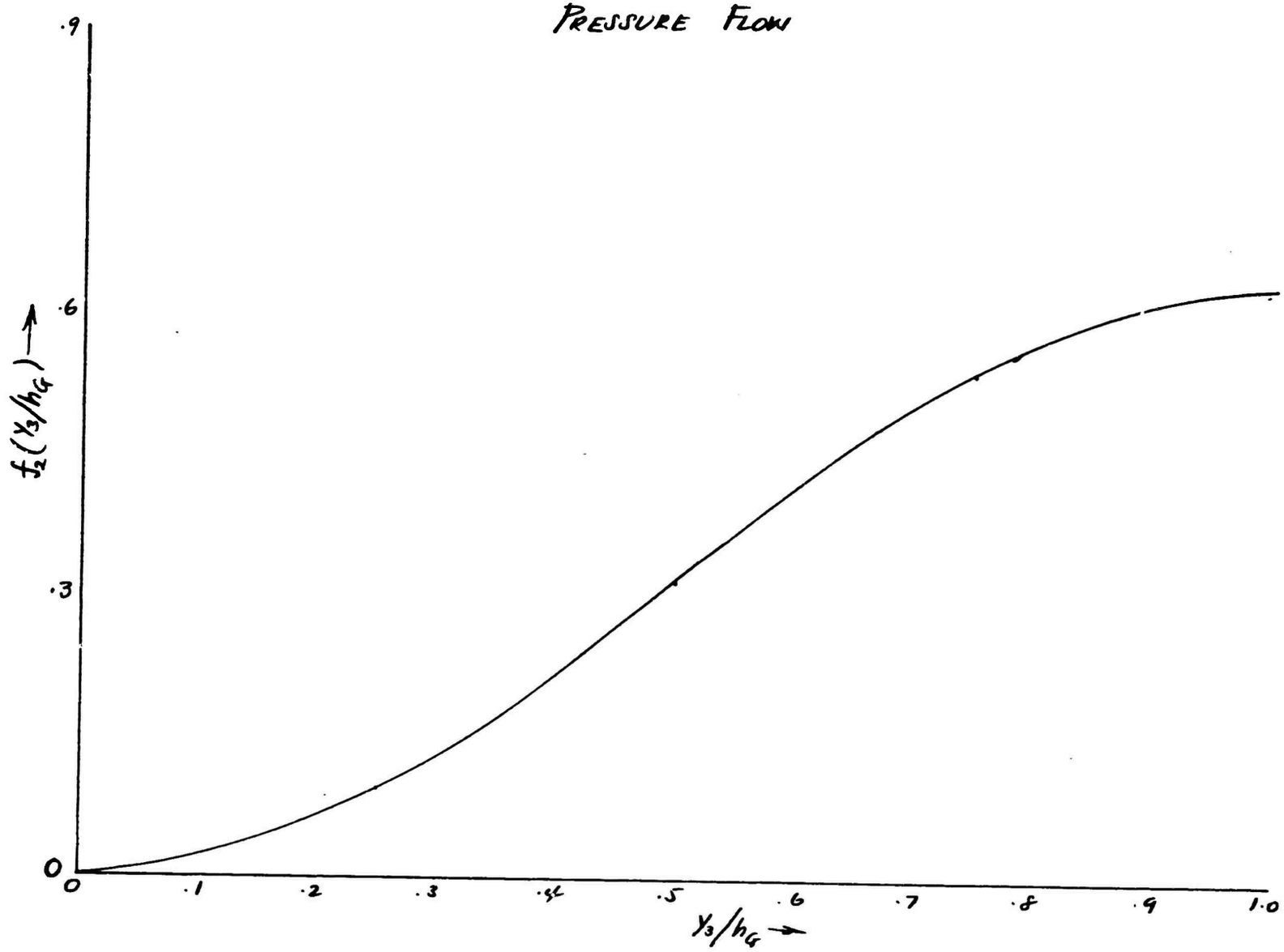

VI EFFECTS OF CHANNEL CURVATURE

It is usually justifiable to treat the flows in the grooves and over the ridges as though they took place between parallel flat plates. However, it is possible for the radius of the screw root, R_1, to be sufficiently different from the radius of the pump barrel, R_0, so that the unwrapping process can introduce some error. This error is, of course, principally associated with the groove.

Booy, in an analysis which will not be repeated here, (1) considered the effect of channel curvature. He treated the case of infinitesmal film thickness over the flights, and presumed an "infinite" groove (or channel) width. Using Stokes' equation, Booy showed that it is possible to obtain a flow-field solution in the following form.

Radial velocity and pressure gradient negligible.

Axial velocity and pressure gradient inter-related as follows:

$$w = \frac{R_0^2}{4\mu}\frac{\partial p}{\partial x_2}\left[\left(\frac{r}{R_0}\right)^2 + (1-\alpha^2)\frac{\ln\left(\frac{r}{R_0}\right)}{\ln\alpha} - 1\right]; \quad \alpha = \frac{R_1}{R_0} \qquad (6.01)$$

Tangential velocity and pressure gradient inter-related as follows:

$$v = \frac{2\pi N}{1-\alpha^2}\left(\frac{r^2-R_1^2}{r}\right) + \frac{r}{2\mu}\frac{\partial p}{\partial \theta}\frac{1}{(1-\alpha^2)}\left[\ln\left(\frac{r}{R_0}\right) - \alpha^2\ln\left(\frac{r}{R_1}\right) - \left(\frac{R_1}{r}\right)^2\ln\alpha\right] \qquad (6.02)$$

The two undetermined pressure derivatives appearing in the foregoing equations were determined by requiring that: (a) the net flow normal to the ridges (or flights) be zero, (b) the volumetric throughput be appropriately related to

the integrated pressure gradient from entrance to exit at ny fixed transverse position in the groove. (Note: all such integrated gradients, or pressure differences, must be the same, although transverse pressure ripples remain to be cancelled by edge corrections.)

In the case of helical grooves, the assumption of "infinite" groove width is justified only when the groove depth is small compared with the screw root radius. Accordingly, it is reasonable to restrict consideration to those cases where the ratio (R_1/R_0) is greater than 0.5 In Appendix B it is proved that a virtually "flat-plate" formula results if a "mean" radius is selected two-thirds of the way from the root to the barrel radius. The helix angle at this mean radius is taken as "β." The simplified formula is:

$$Q = s\,\frac{(1+\frac{\epsilon}{6})}{(1+\frac{\epsilon}{3}\sin^2\beta)}\left[\frac{V_2 h_G}{2} - \frac{h_G^3}{12\mu}\left(\frac{\partial p}{\partial y_2}\right)_{y_1}\right];\quad \epsilon \equiv \frac{h_G}{R_o} \qquad (6.03)$$

This formula shows that within the limits designated, the effective groove width varies by about plus or minus 8%. Fur-

shows that the curvature correction virtually vanishes for a groove angle of 45 degrees.

Booy's solution of Stokes' equation does not yield zero local velocity normal to the groove edges - only zero net flow normal thereto. This same type of average conformity to the velocity boundary condition would be provided by a solution of Reynolds' equation in the case of a more shallow groove. Hence sidewall corrections are in order. Rigorously, such corrections depend on the radius ratio, α. However,

if corrections on corrections are dismissed by reason of their second-order smallness, the analysis of Section V is applicable.

VII EDGE SOLUTIONS FOR RECTANGULAR GROOVING

At this point we revert to further consideration of the entrance-exit edge problem. It suffices to treat this aspect of the pump problem with Reynolds' equation. Moreover, attention will be directed to the special, but extremely important, case of rectangular grooving with equal groove and ridge width.

The analysis of Section III demonstrates that the principal result required from solution of an edge problem is the value of $\tilde{q}_\infty$. Some information concerning this value is provided by the mass-content rule. Thus, integrate eq. (3.01) over one groove-ridge cycle:

$$\left(\frac{\Delta}{L}\right)^2 \frac{d^2}{d\bar{x}^2}\int_0^1 H^3 \tilde{q}\, d\zeta - 2(\cos\beta)\frac{\Delta}{L}\frac{d}{d\bar{x}}\int_0^1 H^3 \frac{\partial \tilde{q}}{\partial \zeta}\, d\zeta - \frac{\Delta}{L}(\cos\beta)\frac{d}{d\bar{x}}\int_0^1 \tilde{q}\frac{dH^3}{d\zeta}\, d\zeta = 0 \tag{7.01}$$

Integration of the second term by parts results in some cancellation, and the following simpler equation.

$$\left(\frac{\Delta}{L}\right)\frac{d^2}{d\bar{x}^2}\int_0^1 H^3 \tilde{q}\, d\zeta + (\cos\beta)\frac{d}{d\bar{x}}\int_0^1 \tilde{q}\frac{dH^3}{d\zeta}\, d\zeta = 0 \tag{7.02}$$

This equation can be integrated once with respect to "$\bar{x}$." The integration constant must be zero if uniformity is to be achieved at infinity. Therefore:

$$\left(\frac{\Delta}{L}\right)\frac{d}{d\bar{x}}\int_0^1 H^3 \tilde{q}\, d\zeta = -(\cos\beta)\int_0^1 \tilde{q}\frac{dH^3}{d\zeta}\, d\zeta \tag{7.03}$$

In the case of rectangular grooving, the film-thickness derivative becomes a delta-function at $\zeta = 0$ and $\zeta = \gamma$. Thus:

$$\left(\frac{\Delta}{L}\right)\frac{d}{d\xi}\int_0^1 H^3\tilde{q}\,d\zeta = \cos\beta\,(H_1^3 - H_2^3)(\tilde{q}_\gamma - \tilde{q}_0) \tag{7.04}$$

It would appear that further progress cannot be made along these lines for the case of arbitrary groove angle, since $\tilde{q}_0$ and $\tilde{q}_\gamma$ depend on both "ξ" and the film-thickness ratio, H_1/H_2. In the special case of $\beta = \pi/2$, it is seen from eq. (7.03) that in all cases:

$$\int_0^1 H^3\tilde{q}\,d\zeta = \text{constant} \tag{7.05}$$

With rectangular grooving (and any β) $\tilde{q}$ must become the saw-tooth function along $\xi = 0$. (See eq. 2.14 and Fig. 3) For convenience, assign unit amplitude (rather than γ) to this function. Then it is easy to show from eq. (7.05) that:

$$\tilde{q}_\infty^1 = 0.5$$

For arbitrary "β", a solution for "$\tilde{q}_\infty$" probably cannot be obtained in closed form, even for rectangular grooves and ridges. However, for an <u>isolated</u> rectangular groove (zero ridge or flight film thickness), the author has been able to obtain such a solution. Details of the analysis are given in Appendix C. The procedure involves transforming by conformal mapping problem A of Fig. 8 into problem B. With constant film thickness, "$\tilde{q}$" satisfies Laplace's equation in the (γ_1, γ_2) plane. By virtue of the properties of conformal mapping, it will also, then, satisfy Laplace's equation in the (u, v)

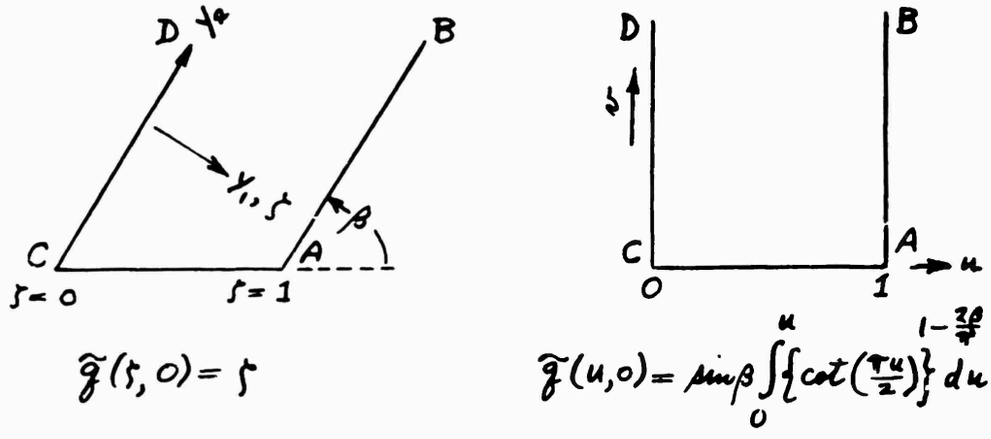

Figure 8 Conformal Transformation

plane. Zero normal derivative along the groove sides is also preserved.

Now the average value of "$\tilde{q}$" at any level v = const. is also "$\tilde{q}^i_\infty$" in the (u,v) plane. However, both planes possess the same "$\tilde{q}^i_\infty$." Therefore, the determination of "$\tilde{q}^i_\infty$" is reduced to an integration along v = 0. The final result is:

$$\tilde{q}^i_\infty = \frac{\tan\beta}{\pi}\left\{\psi\left(\tfrac{1}{2}\right) - \psi\left(\tfrac{\beta}{\pi}\right)\right\} \qquad (7.06)$$

where "ψ" is the Digamma function, tabulated (e.g.) in ref. 7.

In the case of rectangular grooving, the asymptotic value of "$\tilde{q}_\infty$" at the exit can be found from that at the inlet. The inlet and exit configurations, as shown in Fig. 9, are helpful in understanding the relation. The pressure ripples which serve as boundary conditions for the respective "$\tilde{q}_\infty$'s" are shown. Now the "response" to the pressure ripple of the inlet configuration is "$\tilde{q}^i_\infty$." The response to a uniform pressure of unity would be, of course, just 1.0. Because of the linearity and homogeneity of the differential equation for "$\tilde{q}$", the response to (1.0 minus the inlet pressure ripple) would be $1 - \tilde{q}^i_\infty$.

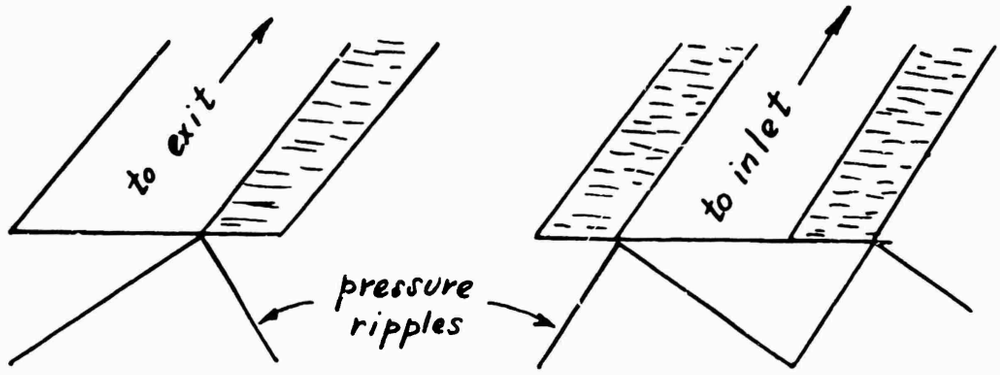

Inlet Configuration Exit Configuration

Figure 9 Sketch to Assist Understanding of Inter-relation of Inlet and Exit $\tilde{q}$'s

However, as can be seen by examining the ripple for the exit configuration, this newly-created compound ripple at the inlet is precisely the same. Therefore:

$$\tilde{g}^{e}_{\infty} = 1 - \tilde{g}^{i}_{\infty} \tag{7.07}$$

In particular, for the isolated rectangular groove:

$$\tilde{g}^{e}_{\infty} = \frac{\tan\beta}{\pi}\left\{\psi(1-\tfrac{\beta}{\pi}) - \psi(\tfrac{1}{2})\right\} \tag{7.08}$$

Reference to eq. (3.05) shows that the difference $\tilde{g}^{i}_{\infty} - \tilde{g}^{e}_{\infty}$ is the quantity needed for over-all pump-performance calculations. Accordingly, this is the quantity presented in Fig. 10 as a function of groove angle and film-thickness ratio. The groove and ridge widths are taken as equal. The curve for $H_2/H_1 = 0$ corresponds to eq. (7.06). The curves for other film-thickness ratios were obtained by use of the finite-element numerical approach developed at The Franklin Institute[8]. For this data the author is much indebted to Dr. T. Y. Chu. Appendix D gives the numerical values on which the curves of Fig. 10 are based. Cross-plotting was employed with the

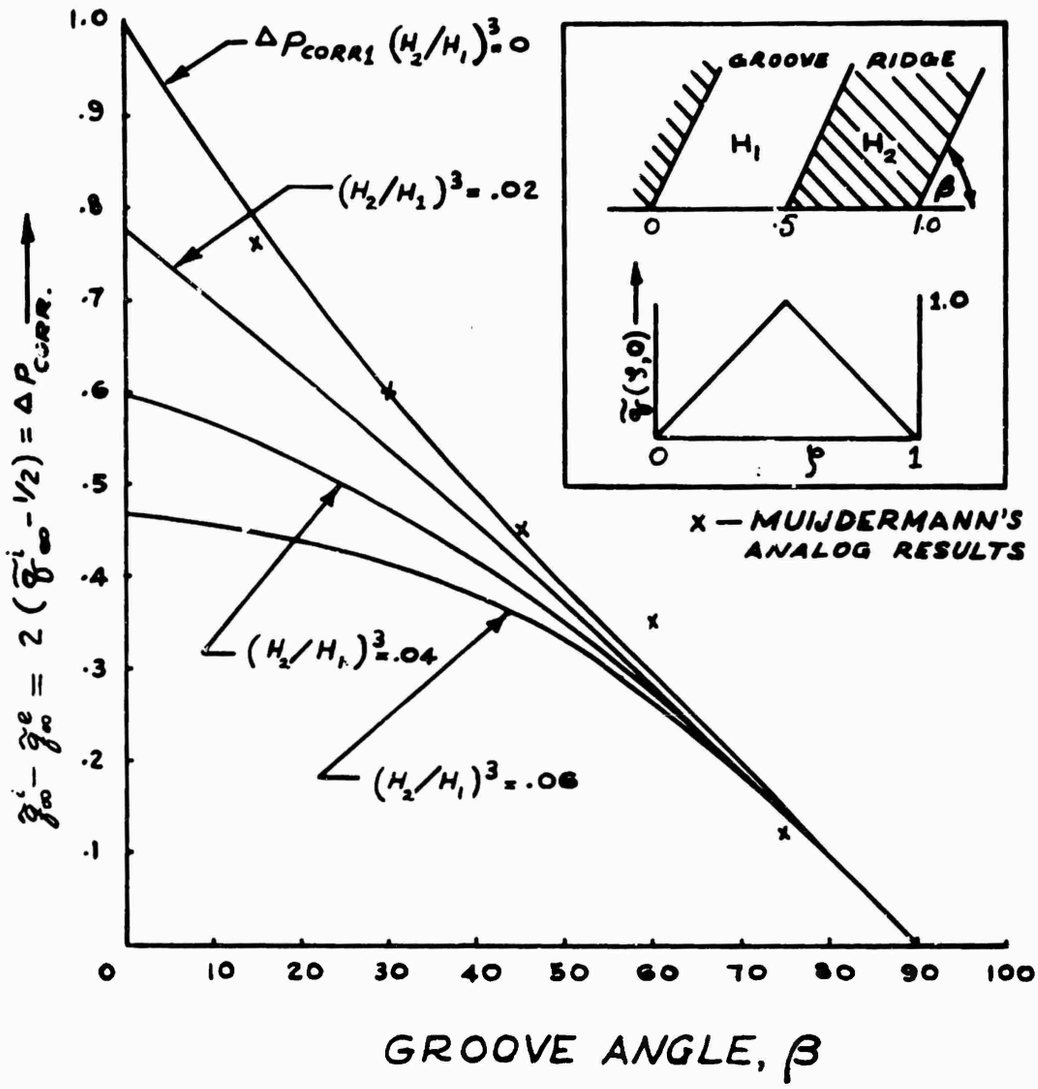

Figure 10 *Pressure Correction Factors for Edge Effect with Rectangular Grooving (Versus Groove Angle)*

assumption of linearity in $(H_2/H_1)^3$.

The asymptotic levels of "$\tilde{q}$" can be found from Fig. 10, but no indication is provided concerning the distance along the groove or channel required to attain them. A reasonable estimate can be formed by further consideration of the case of the isolated groove with $\beta = \pi/2$. In this particular case, a standard Fourier treatment yields:

$$\tilde{q} = \sum_{n=0}^{\infty} A_n \cos(n\pi u)\, e^{-n\pi v} \tag{7.09}$$

Here $A_0 = \overline{\tilde{q}} = \tilde{q}_\infty$. Deviations from uniformity approach zero exponentially, with the least rapid attenuation associated with the first mode, containing the factor $e^{-\pi v}$. When $v = 1$, this factor has already been reduced to only 4.3% of its value on the boundary $v = 0$. Translated into a more general conclusion, this result means that end-effects persist for only about one channel-width into the channel. In the case of oblique channels, measurement towards the interior should be made from the apex of the obtuse angle. To achieve asymptotic conformity within the pump interior, there is a minimum axial length required. It is given by: (approx.)

$$\frac{L}{\Delta} \geq 2\sin\beta + \cos\beta \tag{7.10}$$

VIII COMPARISONS WITH OTHER INVESTIGATIONS

In order to develop a suitable pump-performance formula, it has been necessary to repeat some material presented by earlier investigators. Here an effort will made to indicate the aspects of novelty of the present work, to inter-compare

with earlier results, and to report various checks for accuracy which were made.

Accurate account for cross-flight leakage (within Reynolds' lubrication theory) was made by Whipple,[9] Vohr and Pan[10] and by others treating herringbone-pattern bearings, as well as by Muijdermann[3] in work cited earlier. However, the derivation given in Section II is believed to be new, and is simpler than the matching of solutions at groove-ridge interfacial discontinuities. For the special case of rectangular grooving, eq. (2.14) gives Muijdermann's "approximate pressure distribution."

Exact solutions for established laminar flows have a venerable past. "Pressure-flow" expression (5.03) for a rectangular flow cross-section was given by Carley and Strub[4] as a form preferable to that given by Boussinesq -- although mathematically equivalent. In the same way, expression (5.02) for "drag flow" is somewhat to be preferred to equivalent series given in refs. (1), (4), and elsewhere. In each case, rapid series convergence with attendant computational simplicity is obtained by treating the sidewall flow deficiency as a residual, boundary-layer effect, brought out further by the approximate expressions (5.04) and (5.05). The partial deficiency functions in eqs. (5.06) and (5.07) capitalize on this simplicity.

Booy's analytical results for the influence of channel curvature are reproduced by eq (6.03) in the (h_G/R_0) range of most interest. With virtually the same degree of approximation, his flow factors are given by: (his notation)

$$F_{DC} = \frac{1+\frac{\epsilon}{6}}{1+\frac{\epsilon}{1-\frac{\epsilon}{2}}\sin^2\phi_0} \qquad F_{PC} = \frac{1+\frac{\epsilon}{2}}{1+\frac{\epsilon}{1-\frac{\epsilon}{2}}\sin^2\phi_0} \qquad (8.01)$$

Values from eqs. (8.01) agree adequately with those from Booy's Figs. 3 and 4 of ref. (1). The very worst agreement, corresponding to a radius ratio of 2.0 and extremes of groove angle, is shown below.

	F_{DC} (8.01)	F_{DC} (Booy)	F_{PC} (8.01)	F_{PC} (Booy)
$\phi_o = 5$	1.08	1.07	1.242	1.308
$\phi_o = 60$	0.722	0.693	0.833	0.847

Agreement improves rapidly with diminishing "ϵ".

Both Muijdermann[3] and Booy[2] have dealt with the edge effect at the inlet and exit of an isolated groove. Muijdermann's electrical-analog results are shown on Fig. 10. His results agree with the present exact results within 20%, and the agreement is considerably inside this limit for most measurements. It should be recalled that any deviations here are in a <u>correction</u> term. A less demanding comparison is possible with Booy's finite-difference computations of his pressure-flow correction factor, F_{PE}. This factor satisfies the following relation: (Booy's notation)

$$\frac{1}{F_{PE}} = 1 - \frac{\Delta p_{corr}}{(L_{co}/b_o)\tan\phi_o} \qquad (8.02)$$

Values from this equation are imperceptibly different from those presented in Booy's Fig. 12, where curves for β-values of arctan(1/3,1/2,1) were presented.

For the case of rectangular grooving with $H_2/H_1 \neq 0$, there have hitherto been no accurate corrections available. Muijdermann tentatively offers a formula based on heuristic reasoning. He expresses all pressure corrections in terms of

the pressure correction for an isolated groove. Thus:

$$\Delta p_{corr} = \Delta p_{corr_1} \frac{1 - \left(\frac{H_2}{H_1}\right)^3}{1 + \left(\frac{H_2}{H_1}\right)^3} \qquad (8.03)$$

Although this formula gives correct limiting values at $H_2/H_1 = 0$ and $H_2/H_1 = 1$, it would appear to be considerably in error for some intermediate values. For example, with $\beta = 15^\circ$ and $(H_2/H_1)^3 = 0.06$, Fig. 10 gives $\Delta p_{corr} = 0.43$, whereas eq. (8.03) gives:

$$\Delta p_{corr} = 0.79 \frac{1 - 0.06}{1 + 0.06} = 0.70$$

Actually, the curves in Fig. 10 for $H_2/H_1 \neq 0$ must be regarded as somewhat tentative, inasmuch as the finite-element calculations were not "converged" by running with diminishing grid size. Checks with the exact conformal-mapping solution warrant an error estimate of less than 3%.

IX PUMP PERFORMANCE FORMULA

The individual results of the preceding sections will now be combined to yield the overall relation between pressure difference and quantity pumped. The development will be for one groove-ridge (channel-flight) pair, and it will be assumed that the channel width has been adjusted for curvature prior to "unwrapping" by use of the factor in eq. (6.03).

With reference to Fig. 4, the flow across AC is equal to the flow across AB plus the flow across BC. Now Reynolds' equation is deemed satisfactory for the computation of all flows except that along the groove. (The transverse flow over AB is small, in any event, and the flow along the ridge in-

volves a very small film thickness.) The sidewall flow deficiency in the groove is given by the second (subtractive) terms in eqs. (5.06) and (5.07). Thus the total flow, including sidewall effects, is given by:

$$Q = Q_{Rey} - Q_{def} \tag{9.01}$$

The flows will, of course, be evaluated in the pump interior. Again:

$$Q = Q_{Rey} - \left[\frac{V_2 h_G S F_D}{2} - \frac{h_G^3 S}{12\mu} \left(\frac{\partial p}{\partial y_2} \right)_{y_1} F_P \right] \tag{9.02}$$

The factors F_D and F_P will ordinarily be given well enough by:

$$F_D = \frac{h_G}{S} f_1\left(\frac{y_2}{h_G}\right) \quad ; \quad F_P = \frac{h_G}{S} f_2\left(\frac{y_2}{h_G}\right) \tag{9.03}$$

The required pressure derivative can be put in dimensionless form. Thus:

$$\left(\frac{\partial p}{\partial y_2} \right)_{y_1} = (\sin^2\beta) \frac{6\mu \Delta U_1}{c^2 L} \left(\frac{\partial \pi}{\partial \xi} \right)_{\xi} \tag{9.04}$$

When this derivative is used on the interior pressure solution, given by eq. (2.14), and inserted into eq. (9.02), the result is:

$$Q = Q_{Rey} - \frac{U_1 (\cos\beta)(\gamma\Delta) h_G}{2} \left[F_D - \tan^2\beta \; H_G^3 F_P \right] \tag{9.05}$$

Combination with the Reynolds' flow now gives:

$$Q = -\frac{c(U_1 \cos\beta)\Delta}{2} \left[\alpha \left\{ \frac{1}{\bar{H}^3} + \bar{H}^3 \tan^2\beta - \gamma (\tan^2\beta) H_G^3 F_P \right\} \right. \tag{9.06}$$
$$\left. + \left\{ \frac{\bar{H}^2}{\bar{H}^3} - \bar{H} + \gamma F_D H_G \right\} \right]$$

Further straightforward algebraic rearrangement gives:

$$\frac{Q}{\frac{U_1}{2} c\delta \tan\beta} = \cos^2\beta \left[\left(\bar{H} - \frac{\bar{H}^{-2}}{\bar{H}^{-3}} - r F_D H_G \right) - \alpha \left(\frac{1}{\bar{H}^{-3}} + \bar{H}^3 \tan^2\beta - r F_p H_G^3 \tan^2\beta \right) \right] \quad (9.07)$$

Let us turn now to the pressure-difference expression given by eq. (3.05). The "$\tilde{q}_\infty^i$'s" of this equation must correspond to the ripple term in eq. (2.14), since rectangular grooving is now assumed. For unit sawtooth ripple, Fig. 10 gives:

$$2\tilde{q}_\infty^i - 1 \equiv \Delta P_{corr}$$

Hence, for rectangular grooving, eq. (3.05) becomes:

$$\pi(1) - \pi(0) = \frac{\alpha}{\left(\frac{\Delta}{L}\cos\beta\right)} + (amplitude)\,\Delta P_{corr} \quad (9.08)$$

where the amplitude is:

$$Amplitude = r\left\{ \frac{\left(\bar{H}_1^{-3}\bar{H}^{-2} - \bar{H}^{-3}H_1^{-2}\right) + \alpha\left(H_1^{-3} - \bar{H}^{-3}\right)}{\bar{H}^{-3}} \right\} \quad (9.09)$$

Again, some algebraic rearrangement gives:

$$\frac{c^2 \Delta p}{6\mu L U_1 \tan\beta} = \alpha - \left(\frac{r\Delta}{L}\right)\cos\beta\,\Delta P_{corr} \left[\frac{\alpha\left(\bar{H}^{-3} - H_1^{-3}\right) + \left(\bar{H}^{-3}H_1^{-2} - H_1^{-3}\bar{H}^{-3}\right)}{\bar{H}^{-3}} \right] \quad (9.10)$$

Elimination of the pressure-gradient term "α" between eqs. (9.10) and (9.07) yields the following final pump performance formula. Thus: (with $c = h_G$, so that $H_G = H_1 = 1$)

$$\Delta P^* + \frac{S_2}{S_1} = \left\{ 1 - \frac{r\delta}{L}\cos\beta\sin\beta\,\Delta P_{corr}\, S_1 \right\} \left\{ \frac{S_3}{S_4} + \frac{S_2}{S_1} - \frac{Q^*}{S_4 \cos^2\beta} \right\} \quad (9.11)$$

Here:

$$\Delta P^* = \frac{c^2 \Delta p}{6\mu L U_1 \tan\beta} \quad ; \quad Q^* = \frac{Q}{\frac{U_1}{2} c\delta \tan\beta} \quad (9.12)$$

$$S_1 = 1 - \frac{1}{\bar{H}^{-3}} \quad ; \quad S_2 = 1 - \frac{\bar{H}^{-2}}{\bar{H}^{-3}} \quad (9.13)$$

$$S_3 = \bar{H} - \frac{\bar{H}^{-2}}{\bar{H}^{-3}} - r F_D \; ; \quad S_4 = \frac{1}{\bar{H}^{-3}} + \bar{H}^3 \tan^2\beta - r F_p \tan^2\beta \quad (9.14)$$

X A NUMERICAL EXAMPLE

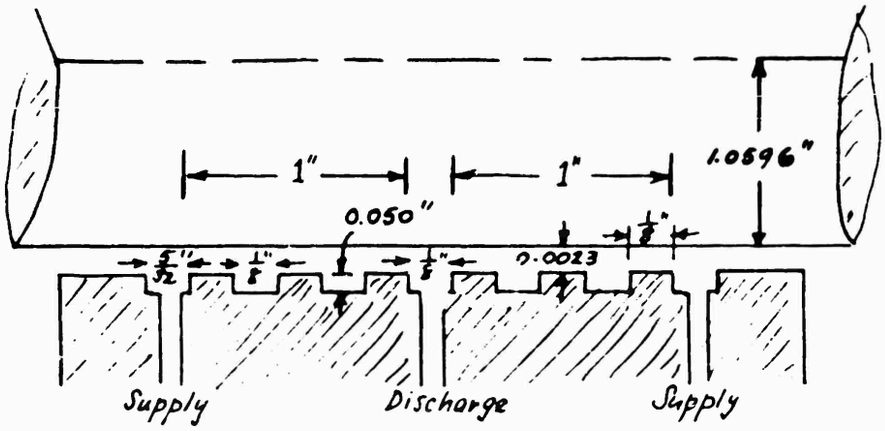

Figure 11 Dimensions of Experimental Screw Pump

The dimensions of an experimental screw pump tested at Columbia University are shown above in Fig. 11. Data for this test were kindly supplied the author by Prof. D. D. Fuller. The pump possesses two single-thread pumping sections working in opposition. The channel-grooving is in the barrel. Pertinent characteristics are listed below.

Pitch of Threads: four per inch

Shaft Diameter: 2.1192 ins.

Barrel Diameter: 2.1238 ins.

Width of Channel: 0.125 ins.

Width of Flights: 0.125 ins.

Depth of Channel Grooving: 0.050 ins.

The corresponding film thicknesses are:

Ridge Film Thickness: h_R = radial clearance = 0.0023 ins.

Groove Film Thickness: h_G = 0.0023 + 0.050 = 0.0523ins.

Also: $H_G = H_1 = 1$ and $H_2 = 0.0023/0.0523 = 0.044$

Unwrapping of Pump Channel

Although, in this instance, the effect of channel curvature

is very small, for the sake of illustration its magnitude will be computed.

$$R_m = 0.5 * 2.1192 + (2/3)* 0.0523 = 1.0945 \text{ ins.}$$

Therefore:

$$\sin\beta = \frac{0.250}{2\pi * 1.0945} = 0.0364 \cong \tan\beta$$

In addition:

$$\epsilon = h_G/R_0 = 0.0523/(0.5*2.1192 + 0.0523) = 0.047$$

The effective groove width is now, according to eq. (6.03),

$$s_{eff} = 0.125\ (1 + 0.047/6) = 0.126$$

Sidewall Factors:

For determination of the factors F_D and F_P, we have:

$$h_G/s = 0.0523/0.126 = 0.415$$

and: $$y_3/h_G = 0.05/0.0523 = 0.956$$

With the definitions in eqs. (9.03) and the use of Figs. 6 and 7, we obtain:

$$F_D = 0.415 * 0.516 = 0.214$$

$$F_P = 0.415 * 0.624 = 0.259$$

Film-Thickness Constants:

The following different averages of film thickness are required.

$$\overline{H} = 0.5\ (1 + 0.044) = 0.522$$

$$\overline{H^3} = 0.5 + 0.5*(0.044)^3 = 0.500$$

$$\overline{H^{-2}} = 0.5 + 0.5/(0.044)^2 = 260$$

$$\overline{H^{-3}} = 0.5 + 0.5/(0.044)^3 = 5865$$

Evaluation of the S_k:

The four S-constants can now be evaluated. Thus:

$$S_1 = 1 - 1/5865 = 1.000$$

$$S_2 = 1 - 260/5865 = 0.955$$

$$S_3 = .522 - 260/5865 - .5*.214 = 0.370$$

$$S_4 = 1/5865 + .5*(.0364)^2 - .5*.259*(.0364)^2$$
$$= 6.62*10^{-4}$$

Final Pump Formula:

Direct substitution into eq. (9.11) now gives the final formula relating operating pressure difference and quantity of liquid being pumped. (Δp_{corr} is read from Fig. 10.) Thus:

$$\Delta P^* + \frac{.955}{1} = \left\{1 - \frac{.5*.252*.975*1*1}{1}\right\}\left\{\frac{.370}{6.62*10^{-4}} + \frac{.955}{1} - \frac{Q^*}{6.62*10^{-4}*1}\right\}$$

Or:

$$\Delta P^* = 488 - 1320\ Q^* \qquad (10.01)$$

It will be observed that the numerical constants in the above formula depend on the geometry only. The speed and the fluid viscosity appear solely in the dimensionless variables ΔP^* and Q^*, and are assignable over wide ranges.

Comparison with Experiment:

In an experiment conducted with the pump of Fig. 11, the following measurements were made:

Shaft Speed: 3000 rpm

Shut-off Pressure: 42.5 psi

Fluid Viscosity: $4.57*10^{-6}$ lb-sec/in^2

The viscosity value was inferred from a viscosity-temperature curve for the oil with measured temperature used as argument.

A prediction of the shut-off pressure is simply made with the use of eq. (10.01) and the definition of ΔP^* in eq. (9.12).

The velocity at the outer radius of the groove (with the shaft treated as stationary) is:

$$U_1 = (3000/60)*3.142*2*1.112 = 348 \text{ in/sec}$$

Then, since:

$$\Delta p = \frac{6\mu L U_i \tan\beta}{c^2} \Delta P^* \qquad (10.02)$$

the prediction of shut-off pressure is:

$$\Delta p = \frac{6*4.15*10^{-6}*1*348*.0364}{(.0523)^2} * 488 = \underline{56.3 \text{ psi}}$$

In a second experiment with the same pump, the data were as follows:

Shaft Speed: 3000 rpm

Flow: 0.525 in^3/sec

Pressure Difference: 31.5 psi

Fluid Viscosity: 4.57 lb-sec/in^2

With the given values of pressure difference and viscosity:

$\Delta P^* = 248$ and $Q^* = (488-248)/1320 = 0.182$

Reversion of the definition of Q^* in eq. (9.12) gives:

$$Q = \frac{U_i}{2} c \delta \tan\beta \, Q^* = \frac{U_i}{2} c \frac{\Delta}{\cos\beta} Q^* \qquad (10.03)$$

Therefore:

$$Q = (348/2)*.0523*(.250/1)*.182 = 0.415 \text{ in}^3\text{/sec}$$

$$= \text{(for two pumping sections) } \underline{0.830 \text{ in}^3\text{/sec}}$$

Compared with the measured values of 42.5 psi and 0.525 in^3/sec for the shut-off pressure and flow, the predictions of 56.3 psi and 0.830 in^3/sec are optimistic. However,

if only cross-flight leakage had been allowed for, with no consideration of channel curvature, sidewall effects, and inlet and exit corrections, the values would have been 62.8 psi and 1.12 in^3/sec. Clearly, consideration of these additional effects greatly improves accord between theory and experiment.

An examination of possible sources of the residual discrepancy leads to the conclusion that the viscosity values employed in the calculations are too high. Such values would arise through measurement of temperatures lower than actually existed in the oil films -- an eventuality which Prof. Fuller suggests as highly likely in the foregoing experiments. In fact, it is noteworthy that if the viscosity values used in the theoretical predictions are arbitrarily lowered by 25%, the predicted shut-off pressure becomes the same as measured, and the predicted flow is a mere 0.025 in3/sec higher than measured.

ACKNOWLEDGMENT

The author is happy to acknowlege the benefit of several discussions of Prof. D. D. Fuller, who also made available unpublished data.

As previously noted, the author is also much indebted to Dr. T. Y. Chu for the finite-element computer runs which provided data for Δp_{corr} when H_2/H_1 is different from zero.

This work was performed under Contract Nonr-2342, jointly sponsored by the Department of Defense, The Atomic Energy Commission and The National Aeronautics and Space Administration, and monitored by Mr. S. Doroff of the Fluid Dynamics Branch of the Office of Naval Research.

References:

1. Booy, M. L., "Influence of Channel Curvature on Flow, Pressure Distribution, and Power Requirements of Screw Pumps and Melt Extruders," Trans. A. S. M. E., Jnl. of Engrg. for Industry, Vol. 86, Series B, pp. 22-30, (1964).
2. Booy, M. L., "Influence of Oblique Channel Ends on Screw-Pump Performance," Trans. A. S. M. E., Jnl. of Basic Engrg., Vol. 88, Series D, pp. 121-131, (1966).
3. Muijdermann, E. A., "Spiral-Groove Bearings," Thesis, Technological Univ., Delft, The Netherlands, (1964). Published as Philips Research Report Supplement No. 2. Available from Philips Technical Library, Springer-Verlag, N. Y., (1966), 199 pages. See also: "Analysis and Design of Spiral-Groove Bearings," Trans. A. S. M. E., Jnl. of Lubrication Technology, Vol. 89, Series F, pp. 291-306, (1967).
4. Carley, J. F. and Strub, R. A., "Basic Concepts of Extrusion," Indus. and Engrg. Chemistry, Vol. 45, No. 1, pp. 970-3, (1953).
5. Carley, J. F., Mallouk, R. S. and McKelvey, J. M., "Simplified Flow Theory for Screw Extruders," Indus. and Engrg. Chemistry, Vol. 45, No. 1, pp. 974-8, (1953).
6. Pigott, W. T., "Pressures Developed by Viscous Materials in the Screw Extrusion Machine," Trans. A. S. M. E., Vol. 73, pp. 947-955, (1951).

7. "Handbook of Mathematical Functions," National Bureau of Standards, Applied Mathematics Series 55, June 1964. For sale by the Supt. of Documents, U. S. Gov't. Printing Office, Wash., D. C., 20402.

8. Reddi, M., "Finite Element Solution of the Incompressible Lubrication Problem," to be published in Journal of Lubrication Technology, Trans. A. S. M. E., (1969).

9. Whipple, R. T. P., "Herringbone-Pattern Thrust Bearing," Atomic Energy Research Establishment, Harwell, Berkshire, England. T/M 29, (1951).

10. Vohr, J. H., and Pan, C. H. T., "On the Spiral-Grooved, Self-Acting, Gas Bearing," Mechanical Technology, Inc., Latham, N. Y. MTI Technical Report MTI 6352, prepared under O. N. R. Contract Nonr-3730(00), Task NR 061-131, (1963).

11. "Smithsonian Mathematical Formulae and Tables of Elliptic Functions," by E. P. Adams and R. L. Hippisley, publication 2672, Wash., D. C., 1939. Published by the Smithsonian Institution.

APPENDIX A

SIDEWALL EFFECTS

It is convenient to solve eq. (5.01) in terms of dimensionless variables:

$$\tau = \frac{y_1}{h_G} \; ; \; \eta = \frac{y_3}{h_G}$$

Then:

$$\nabla^2_{\tau,\eta} v_2 = -\frac{h_G^2}{\mu} \frac{\partial p}{\partial y_2} \tag{A.01}$$

A particular solution is provided by Reynolds' equation. Thus:

$$v_p = V_2 \eta - \frac{h_G^2}{2\mu} \frac{\partial p}{\partial y_2} (\eta^2 - \eta) \tag{A.02}$$

A homogeneous solution for "v_2" must now be found which vanishes on $\eta = 0$ and 1. This solution is formed from the series:

$$v_H = \sum_{k=1}^{\infty} A_k \sin(k\pi\eta) F_k(\tau) \tag{A.03}$$

where:

$$F_k(\tau) = \frac{\cosh\{k\pi(\tau - \frac{s}{2h_G})\}}{\cosh(\frac{k\pi s}{2h_G})} \tag{A.04}$$

On $\tau = 0$ and 1:

$$\sum_{k=1}^{\infty} A_k \sin(k\pi\eta) = V_2 \eta - \frac{h_G^2}{2\mu} \frac{\partial p}{\partial y_2} (\eta^2 - \eta) \tag{A.05}$$

Then:

$$v_H = V_2 (\frac{2}{\pi}) \sum_{k=1}^{\infty} \frac{(-1)^{k+1}}{k} \sin(k\pi\eta) F_k(\tau) \Big)$$

$$- \frac{h_G^2}{2\mu} \frac{\partial p}{\partial y_2} \frac{4}{\pi^3} \sum_{k=1}^{\infty} \{1 - (-1)^k\} \frac{1}{k^3} \sin(k\pi\eta) F_k(\tau) \tag{A.06}$$

Since v_H must be subtracted from v_p to give the true v_2, it

represents the velocity deficiency occasioned by the sidewalls.

The flow deficiency per unit distance along one sidewall is given by:

$$h_G \int_0^{\frac{s}{2h_G}} v_H \, d\tau = V_2 h_G \frac{2}{\pi^2} \sum_{k=1}^{\infty} \frac{(-1)^{k+1}}{k^2} \sin(k\pi\eta) \tanh\left(\frac{k\pi s}{2h_G}\right) \Bigg)$$

$$- \frac{h_G^3}{2\mu} \frac{\partial p}{\partial y_2} \frac{4}{\pi^4} \sum_{k=1}^{\infty} \left\{1 - (-1)^k\right\} \frac{\sin(k\pi\eta) \tanh\left(\frac{k\pi s}{2h_G}\right)}{k^4} \qquad \text{(A.07)}$$

The total flow deficiency for one sidewall is:

$$h_G^2 \int_0^{\frac{s}{2h_G}} \int_0^1 v_H \, d\tau \, d\eta = V_2 h_G^2 \frac{4}{\pi^3} \sum_{k=1,3,5\ldots}^{\infty} \frac{\tanh\left(\frac{k\pi s}{2h_G}\right)}{k^3} \Bigg)$$

$$- \frac{h_G^4}{2\mu} \frac{\partial p}{\partial y_2} \frac{16}{\pi^5} \sum_{k=1,3,5}^{\infty} \frac{\tanh\left(\frac{k\pi s}{2h_G}\right)}{k^5} \qquad \text{(A.08)}$$

When this last result is multiplied by two, and subtracted from the usual Reynolds flow, eqs. (5.02) and (5.03) are the consequences.

As stated in the main text, when h_G/s is less than 3/4, sidewall effects are essentially confined to the channel ends. For this case, all the hyperbolic tangents in the foregoing series can be taken as unity. Accordingly, let us make this simplification and compute next the <u>partial</u> flow deficiency:

$$2h_G^2 \int_0^{\frac{y_2}{h_G}} \int_0^{\frac{s}{2h_G}} v_H \, d\tau \, d\eta = \frac{V_2}{2} h_G^2 f_1\left(\frac{y_2}{h_G}\right) - \frac{h_G^4}{12\mu} \frac{\partial p}{\partial y_2} f_2\left(\frac{y_2}{h_G}\right) \qquad \text{(A.09)}$$

Then:

$$f_1\left(\frac{y_2}{h_G}\right) = \frac{8}{\pi^3} \sum_{k=1}^{\infty} \frac{(-1)^{k+1}}{k^2} \left\{1 - \cos(k\pi\eta)\right\} \qquad \text{(A.10)}$$

and:

$$f_2\left(\frac{V_2}{h_G}\right) = \frac{48}{\pi^5}\sum_{k=1}^{\infty}\frac{\{1-(-1)^k\}}{k^5}\{1-\cos(k\pi\eta)\} \qquad (A.11)$$

The series for f_2 converges exceedingly rapidly, and can be used for computation directly, with the results shown in Fig. 7. The series for f_1 is best converted, as follows. From ref. 11, p. 139, we have:

$$\frac{1}{2}\ln(1-2r\cos x+r^2) = \sum_{k=1}^{\infty}\frac{r^k\cos(kx)}{k} \qquad (A.12)$$

Setting r = -1, and performing two integrations, one finds:

$$\int_0^x\int_0^x \ln\{2\cos(\tfrac{x}{2})\}\,dx\,dx = \sum_{k=1}^{\infty}(-1)^{k+1}\frac{\{1-\cos(kx)\}}{k^3} \qquad (A.13)$$

Again, from ref. 11, p. 123:

$$\ln(\cos x) = -\sum_{k=1}^{\infty}\frac{2^{2k-1}(2^{2k}-1)B_k}{k(2k)!}x^{2k} \qquad (A.14)$$

where the B_k are the Bernoulli numbers, a few of which are given below.

$B_1 = 1/6$; $B_2 = 1/30$; $B_3 = 1/42$; $B_4 = 1/30$; $B_5 = 5/66$ .....

The integrations of eq. (A.13) are readily performed with the new series, and the result is:

$$\sum_{k=1}^{\infty}(-1)^{k+1}\frac{\{1-\cos(kx)\}}{k^3} = \frac{x^2}{2}(\ln 2) - \sum_{k=1}^{\infty}\frac{(2^k-1)B_k}{2k(2k+2)!}x^{2k+2} \quad ;0\le x\le\pi \qquad (A.15)$$

Finally:

$$f_1(\eta) = \frac{8}{\pi^3}\left[\frac{\pi^2}{2}(\ln 2) - \frac{\pi^4}{96}\eta^4 - \frac{\pi^6}{5760}\eta^6 - \frac{\pi^8}{161280}\eta^8 \ldots\right] \qquad (A.16)$$

This function is graphed in Fig. 6.

APPENDIX B

CHANNEL CURVATURE EFFECTS

Booy (1) gives the following formula for the flow, Q, in terms of the overall pressure difference, P_0, the radius ratio, $\alpha = R_1/R_0$, and other variables.* Thus:

$$Q = R_0^3 N S(\phi_0, \alpha) - R_0^4 T(\phi_0, \alpha) \frac{P_0}{4\mu L} \qquad (B.01)$$

Here:

$$S = \frac{2\pi^2 F(\alpha) K(\alpha) \tan^2\phi_0}{F(\alpha) - 2G(\alpha)\tan^2\phi_0} \; ; \; T = \frac{\pi F(\alpha) G(\alpha) \tan^2\phi_0}{F(\alpha) - 2G(\alpha)\tan^2\phi_0} \qquad (B.02)$$

$$F(\alpha) = (\alpha^2 - 1)\left[(1+\alpha^2) + \frac{1-\alpha^2}{\ln\alpha}\right] \qquad (B.03)$$

$$G(\alpha) = (1-\alpha^2)\left[1 - \left(\frac{2\alpha \ln\alpha}{1-\alpha^2}\right)^2\right] \qquad (B.04)$$

$$K(\alpha) = 1 + \frac{2\alpha^2 \ln\alpha}{(1-\alpha^2)} \qquad (B.05)$$

In succeeding manipulations, use will be made of the fact that:

$$h = R_0 - R_1 \; ; \; R\tan\phi = R_0 \tan\phi_0 \quad \text{for any R} \qquad (B.06)$$

---

*Booy's notation used in this Appendix. A factor of 4 has been introduced into the denominator of the second term of (B.01) to correct for misprint in (1).

Further, y_2 is chosen as distance parallel to the flights at radius, R, and V_2 as the corresponding component of barrel velocity.

Algebraic rearrangements and substitutions give successively:

$$Q = \frac{R_o^2 2\pi F(\alpha) \tan\phi_o}{\{F(\alpha) - 2G(\alpha)\tan^2\phi_o\}} \left[\frac{2\pi R_o N K(\alpha)}{2} - \frac{R_o^2 G(\alpha)\tan\phi_o}{(2/3)} \frac{P_o}{12\mu L_1}\right] \quad (B.07)$$

$$Q = \frac{2\pi R_o R \tan\phi F(\alpha) K(\alpha)}{(1-\alpha)\{F(\alpha) - 2G(\alpha)\tan^2\phi_o\}} \left[\frac{2\pi R_o N(1-\alpha)}{2} - \frac{R\tan\phi R_o G(\alpha)(1-\alpha)}{(2/3)K(\alpha)} \frac{P_o}{12\mu L_1}\right] \quad (B.08)$$

$$Q = \frac{2\pi R \tan\phi \sec\phi F(\alpha) K(\alpha)}{(1-\alpha)\{F(\alpha) - 2G(\alpha)\tan^2\phi_o\}} \left[\frac{V_2 h}{2} - \left\{\frac{R R_o^2 G(\alpha)(1-\alpha)}{(2/3)K(\alpha)}\right\} \frac{1}{12\mu} \frac{\partial p}{\partial y_2}\right] \quad (B.09)$$

Equation (B.09) is valid for any "R." Let us choose R_m to effect, as much as possible, correspondence with standard flat-plate formulas. Thus, take:

$$\frac{R_m R_o^2 G(\alpha)(1-\alpha)}{(2/3)K(\alpha)} \equiv R_o^3 (1-\alpha)^3 = h^3 \quad (B.10)$$

Or:

$$\frac{R_m}{R_o} = \frac{(\frac{2}{3})(1-\alpha)^2 K(\alpha)}{G(\alpha)} \quad (B.11)$$

Because, in most practical circumstances, "α" can never deviate much from unity, it is helpful to write: $\epsilon \equiv 1-\alpha$ and to expand the various functions of "α" in terms of "ϵ". Thus:

$$F(\alpha) = -\frac{4}{3}\epsilon^3\left(1 - \frac{\epsilon}{2}\right); \quad G(\alpha) = \frac{2}{3}\epsilon^3\left(1 + \frac{\epsilon}{2}\right); \quad K(\alpha) = \epsilon\left(1 + \frac{\epsilon}{6}\right) \quad (B.12)$$

$$\frac{R_m}{R_o} = 1 - \frac{\epsilon}{3} \tag{B.13}$$

Formulas (B.12) are very satisfactory approximations for the practical range of "α". For example, even when $R_1/R_2 = 1/2$ ($\alpha = 1/2$), the exact and approximate values of these functions differ little. (See the table below.)

	Exact	Approx.
F(.5)	-.126	-.125
G(.5)	0.108	0.104
K(.5)	0.538	0.543

Use of eq. (B.11) in eq. (B.09) gives:

$$Q = \frac{2\pi R_m \sin\phi \left\{ \frac{V_2 h}{2} - \frac{h^3}{12\mu} \frac{\partial p}{\partial y_2} \right\}}{\cos^2\phi \frac{(1-\alpha)}{K(\alpha)} \left\{ 1 - \frac{2G(\alpha)}{F(\alpha)} \left(\frac{R_m}{R_o}\right)^2 \tan^2\phi \right\}} \tag{B.14}$$

When the ϵ-approximations are used, the following simple equivalent flat-plate formula results:

$$Q = \frac{2\pi R_m \sin\phi_m \left\{ \frac{V_2 h}{2} - \frac{h^3}{12\mu} \frac{\partial p}{\partial y_2} \right\} \left(1 + \frac{\epsilon}{6}\right)}{1 + \frac{\epsilon}{3} \sin^2\phi_m} \tag{B.15}$$

APPENDIX C

SINGLE-GROOVE EDGE CORRECTION

The mapping function

$$w = \frac{\sin\beta}{\pi} \int_0^z z^{\frac{\beta}{\pi}-1} (z-1)^{-\frac{\beta}{\pi}} e^{i\beta}\, dz \equiv \zeta + i\eta$$

converts the real axis of the z-plane into the form shown below in the w-plane

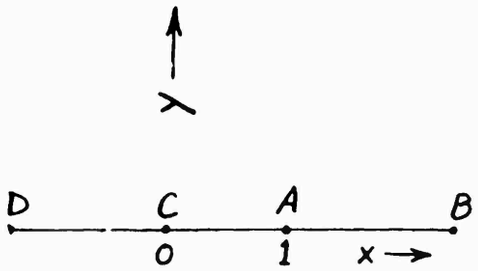

z-plane

$z = x + iy$

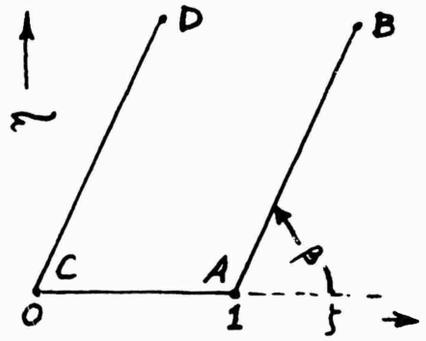

w-plane

$w = (1-\zeta) + i\eta$

When $\beta = \frac{\pi}{2}$ we take $\zeta = u$, $\eta = v$

Along $y = 0$

$$\zeta = \frac{\sin\beta}{\pi} \int_0^x x^{\frac{\beta}{\pi}-1} (1-x)^{-\frac{\beta}{\pi}} dx; \quad u = \frac{2}{\pi} \tan^{-1}\sqrt{\frac{x}{1-x}}$$

Now in the (u, v) plane

$$\tilde{q}_\infty = \int_0^1 \tilde{q}(u)\,du = \tilde{q}(1) - \int_0^1 u \frac{d\tilde{q}}{du}\,du$$

$$= 1 - \int_0^1 u \frac{d\tilde{q}}{du}\,du$$

$$= 1 - \frac{2}{\pi}\int_0^1 \tan^{-1}\sqrt{\frac{x}{1-x}}\,\frac{\sin\beta}{\pi}\,x^{\frac{\beta}{\pi}-1}(1-x)^{-\frac{\beta}{\pi}}\,dx$$

[Note: $\tilde{q} = \int$]

Next let $$x = \frac{t^2}{1+t^2}\;;\quad t = \sqrt{\frac{x}{1-x}}$$

then:

$$\tilde{q}_\infty = 1 - \frac{2(\sin\beta)}{\pi^2}\int_0^\infty \tan^{-1}(t)\; t^{\frac{2\beta}{\pi}-1}\,\frac{2\,dt}{1+t^2}$$

Write $\tan^{-1}(t)$ in the following integral form. Thus:

$$\tan^{-1}(t) = t\int_0^1 \frac{ds}{1+t^2s^2}$$

$$\therefore\ \tilde{q}_\infty = 1 - \frac{2(\sin\beta)}{\pi^2}\int_{s=0}^{1} 2\int_{t=0}^{\infty} \frac{t^{\frac{2\beta}{\pi}}\,dt}{(1+t^2s^2)(1+t^2)}\,ds$$

Resolution into partial fractions gives:

$$\tilde{q}_\infty = 1 - \frac{\sin\beta}{\pi^2}\int_{s=0}^{1} 2 \int_0^\infty \left\{ \frac{1}{(1-s^2)}\frac{1}{(1+t^2)} - \frac{s^2}{1-s^2}\frac{1}{1+t^2s^2} \right\} t^{\frac{2\beta}{\pi}} dt\, ds$$

Use is made of the infinite integral

$$\int_0^\infty \frac{t^{m-1}}{(1+t)^{m+n}}\, dt = \frac{\Gamma(m)\,\Gamma(n)}{\Gamma(m+n)}$$

and the reflection formula for the Gamma function:

$$\Gamma(n)\,\Gamma(1-n) = \frac{\pi}{\sin(n\pi)}$$

Then:

$$\tilde{q}_\infty = 1 - \frac{2\tan\beta}{\pi}\int_0^1 \frac{(1-s^m)}{(1-s^2)}\, ds \;;\quad m = 1 - \frac{2\beta}{\pi}$$

The above definite integral converges, but not with the terms 1, s^m treated separately. Accordingly, the behavior of an integral with the denominator "shaded" to $(1-s^2)^{\frac{1-n}{2}}$ will first be examined.

$$I \equiv \int_0^1 \frac{(1-s^m)}{(1-s^2)^{\frac{1-n}{2}}}\, ds = \frac{1}{2}\left[B\left(\tfrac{1}{2}, \tfrac{n+1}{2}\right) - B\left(\tfrac{m+1}{2}, \tfrac{n+1}{2}\right)\right]$$

$$= \frac{\Gamma\left(\frac{n+1}{2}\right)}{2}\left[\frac{\Gamma\left(\frac{1}{2}\right)}{\Gamma\left(\frac{n+1}{2}+\frac{1}{2}\right)} - \frac{\Gamma\left(\frac{m+1}{2}\right)}{\Gamma\left(\frac{n+1}{2}+\frac{m+1}{2}\right)}\right]$$

Let $\theta = \frac{n+1}{2}$, and examine "I" as $\theta \to 0$.

$$I = \frac{1}{2} \frac{\theta \Gamma(\theta)}{\Gamma(\theta+\frac{1}{2})\Gamma(\theta+\frac{m+1}{2})} \left[\frac{\Gamma(\frac{1}{2})\Gamma(\theta+\frac{m+1}{2}) - \Gamma(\frac{m+1}{2})\Gamma(\theta+\frac{1}{2})}{\theta} \right]$$

$$\longrightarrow \frac{1}{2} \frac{1}{\Gamma(\frac{1}{2})\Gamma(\frac{m+1}{2})} \left[\Gamma(\tfrac{1}{2})\Gamma'(\tfrac{m+1}{2}) - \Gamma(\tfrac{m+1}{2})\Gamma'(\tfrac{1}{2}) \right]$$

Hence:

$$\tilde{q}_\infty = 1 - \frac{\tan\beta}{\pi} \left[\frac{\Gamma'(1-\frac{\beta}{\pi})}{\Gamma(1-\frac{\beta}{\pi})} - \frac{\Gamma'(\frac{1}{2})}{\Gamma(\frac{1}{2})} \right]$$

$$1 - \frac{\tan\beta}{\pi} \left\{ \psi(1-\tfrac{\beta}{\pi}) - \psi(\tfrac{1}{2}) \right\}$$

More conveniently for computation:

$$\tilde{q}_\infty = 1 - \frac{\tan\beta}{\pi} \left\{ \psi(2-\tfrac{\beta}{\pi}) - \psi(\tfrac{1}{2}) - \frac{1}{(1-\frac{\beta}{\pi})} \right\}$$

UNCLASSIFIED
Security Classification

DOCUMENT CONTROL DATA - R&D

(Security classification of title, body of abstract and indexing annotation must be entered when the overall report is classified)

1 ORIGINATING ACTIVITY (Corporate author) The Franklin Institute Research Laboratories Philadelphia, Penna. H. G. Elrod	2a. REPORT SECURITY CLASSIFICATION UNCLASSIFIED 2b GROUP NONE

3 REPORT TITLE

An Analysis of the Side-Leakage Effect in High-Speed Gas Lubricated Slider and Partial ARC Bearings

4. DESCRIPTIVE NOTES (Type of report and inclusive dates)

Interim Report I-C2049-32, March 1969

5 AUTHOR(S) (Last name, first name, initial)

Elrod, H. G.

6. REPORT DATE	7a. TOTAL NO. OF PAGES	7b. NO. OF REFS
March 1969	56	11

8a. CONTRACT OR GRANT NO. Nonr-2342 b. PROJECT NO. c. Task NR 062-316 d.	9a. ORIGINATOR'S REPORT NUMBER(S) I-A2049-32 9b. OTHER REPORT NO(S) (Any other numbers that may be assigned this report) ----

10. AVAILABILITY/LIMITATION NOTICES

Reproduction in whole or in part is permitted for any purpose of the U.S. Government.

11. SUPPLEMENTARY NOTES	12. SPONSORING MILITARY ACTIVITY
	Department of Defense Atomic Energy Commission National Aeronautics & Space Administration

13. ABSTRACT

Recently-performed analysis for herringbone thrust bearings has been incorporated into the theory of the viscous screw pump for Newtonian fluids. In addition, certain earlier corrections for sidewall and channel curvature effects have been simplified. The result is a single, refined formula for the prediction of the pressure-flow relation for these pumps.

To provide a self-contained presentation, some of the results of FIRL Interim Report I-A2049-32 are also given here.

DD FORM 1 JAN 64 1473

UNCLASSIFIED
Security Classification

UNCLASSIFIED
Security Classification

14. KEY WORDS	LINK A		LINK B		LINK C	
	ROLE	WT	ROLE	WT	ROLE	WT
Theory, Analysis						
Viscous Pump						
Pump						
Screw Pump						
Herring Bone Thrust Bearing						
Thrust Bearing						
Hydrodynamic Bearing						
Newtonian Fluid Lubricant						
Sidewall Corrections						
Channel Curvature Corrections						
Pressure Distribution						
Flow Rates						
Edge Correction						
Pump Performance						

INSTRUCTIONS

1. ORIGINATING ACTIVITY: Enter the name and address of the contractor, subcontractor, grantee, Department of Defense activity or other organization *(corporate author)* issuing the report.

2a. REPORT SECURITY CLASSIFICATION: Enter the overall security classification of the report. Indicate whether "Restricted Data" is included. Marking is to be in accordance with appropriate security regulations.

2b. GROUP: Automatic downgrading is specified in DoD Directive 5200.10 and Armed Forces Industrial Manual. Enter the group number. Also, when applicable, show that optional markings have been used for Group 3 and Group 4 as authorized.

3. REPORT TITLE: Enter the complete report title in all capital letters. Titles in all cases should be unclassified. If a meaningful title cannot be selected without classification, show title classification in all capitals in parenthesis immediately following the title.

4. DESCRIPTIVE NOTES: If appropriate, enter the type of report, e.g., interim, progress, summary, annual, or final. Give the inclusive dates when a specific reporting period is covered.

5. AUTHOR(S): Enter the name(s) of author(s) as shown on or in the report. Enter last name, first name, middle initial. If military, show rank and branch of service. The name of the principal author is an absolute minimum requirement.

6. REPORT DATE: Enter the date of the report as day, month, year; or month, year. If more than one date appears on the report, use date of publication.

7a. TOTAL NUMBER OF PAGES: The total page count should follow normal pagination procedures, i.e., enter the number of pages containing information.

7b. NUMBER OF REFERENCES: Enter the total number of references cited in the report.

8a. CONTRACT OR GRANT NUMBER: If appropriate, enter the applicable number of the contract or grant under which the report was written.

8b, 8c, & 8d. PROJECT NUMBER: Enter the appropriate military department identification, such as project number, subproject number, system numbers, task number, etc.

9a. ORIGINATOR'S REPORT NUMBER(S): Enter the official report number by which the document will be identified and controlled by the originating activity. This number must be unique to this report.

9b. OTHER REPORT NUMBER(S): If the report has been assigned any other report numbers *(either by the originator or by the sponsor)*, also enter this number(s).

10. AVAILABILITY/LIMITATION NOTICES: Enter any limitations on further dissemination of the report, other than those imposed by security classification, using standard statements such as:

(1) "Qualified requesters may obtain copies of this report from DDC."

(2) "Foreign announcement and dissemination of this report by DDC is not authorized."

(3) "U. S. Government agencies may obtain copies of this report directly from DDC. Other qualified DDC users shall request through _____."

(4) "U. S. military agencies may obtain copies of this report directly from DDC. Other qualified users shall request through _____."

(5) "All distribution of this report is controlled. Qualified DDC users shall request through _____."

If the report has been furnished to the Office of Technical Services, Department of Commerce, for sale to the public, indicate this fact and enter the price, if known.

11. SUPPLEMENTARY NOTES: Use for additional explanatory notes.

12. SPONSORING MILITARY ACTIVITY: Enter the name of the departmental project office or laboratory sponsoring *(paying for)* the research and development. Include address.

13. ABSTRACT: Enter an abstract giving a brief and factual summary of the document indicative of the report, even though it may also appear elsewhere in the body of the technical report. If additional space is required, a continuation sheet shall be attached.

It is highly desirable that the abstract of classified reports be unclassified. Each paragraph of the abstract shall end with an indication of the military security classification of the information in the paragraph, represented as *(TS)*, *(S)*, *(C)*, or *(U)*.

There is no limitation on the length of the abstract. However, the suggested length is from 150 to 225 words.

14. KEY WORDS: Key words are technically meaningful terms or short phrases that characterize a report and may be used as index entries for cataloging the report. Key words must be selected so that no security classification is required. Identifiers, such as equipment model designation, trade name, military project code name, geographic location, may be used as key words but will be followed by an indication of technical context. The assignment of links, roles, and weights is optional.